DOI: https://doi.org/10.37434/tpwj2024.06.04

EFFECTIVENESS OF THE INFLUENCE OF SOLID-STATE LASER RADIATION ON THE PROCESS OF PULSED-ARC WELDING OF ALUMINIUM ALLOY 1561

Y. Zhao, X. Wang, Z. Liu, V.Yu. Khaskin

Guangdong Provincial Key Laboratory of Advanced Welding Technology, China-Ukraine Institute of Welding, Guangdong Academy of Sciences, Guangzhou, 510650, China

ABSTRACT

The results of consumable electrode pulsed-arc welding of 1561 aluminium alloy of 6 mm thickness (P-MIG) with and without addition of focused radiation of the Nd:YAG laser were analyzed. During laser-P-MIG welding, the influence of the arc energy source improves absorption of laser radiation and promotes high-quality formation of the weld reinforcement, and the influence of the laser source leads to an increase in the depth of penetration due to the formation of a vapour-gas channel (keyhole) and to a decrease in the current density of the anode region of the arc on the electrode wire, which reduces emissions of welding aerosols. Factors influencing the effectiveness of laser radiation during laser-P-MIG welding were determined. It is shown that an increase in laser power leads to an increase in arc voltage with a simultaneous decrease in welding current. Formation of high-quality welds by P-MIG welding of 1561 alloy requires an energy input of 4.5–5.0 kJ/cm. Here, a regular structure of the weld metal with the dendritic parameter of 13–15 μm and joint strength of 90–92 % of the strength of the base metal is formed. Introduction of focused radiation of a 3.0 kW Nd:YAG laser into the welding process allows reducing the energy input by approximately half, due to which the dendritic parameter decreases to 10 μm, and the strength of the joints increases to 93–96 % of base metal strength.

KEYWORDS: aluminium alloy, consumable electrode pulsed arc welding (P-MIG), Nd:YAG-laser radiation, modes, welding aerosols, structures, strength.

INTRODUCTION

ANALYSIS OF PUBLISHED DATA AND PROBLEM DEFINITION

The question of welding aluminium alloy structures is becoming ever more urgent in connection with increasing demand for lightweight vehicles and technical facilities, instruments, etc. [1]. This is also promoted by application of a wide range of building structures from aluminium alloys [2]. In particular, the researchers are interested in application of aluminium alloys of the fourth, fifth and sixth series as building and structural materials [3]. These alloys are attractive not only due to such characteristics as wear- and corrosion resistance, a combination of low density with an acceptable strength, but also due to sufficiently good weldability [4]. Technologies of welding structures from such materials have been optimized for a rather long time [5]. With emergence of modern welding processes, however, in particular laser-arc and laser-plasma [6], there comes the question of improvement of the effectiveness of joining the already well-known materials.

Application of laser-MIG process can be more advantageous for welding aluminium alloys than use of laser-TIG and laser-plasma processes, due to a higher adaptability-to-fabrication of feeding additional material at weld formation and simpler controllability of its structure formation. However, the laser-MIG welding process has its features. So, in this process of welding 5 mm 5083 alloy with application of fiber-laser radiation, a susceptibility to formation of coarse porosity in the welds was revealed [7]. It was related to disturbance of the vapour-gas channel (keyhole) stability. Transition to heat conduction welding mode, which prevents keyhole formation, can help eliminate this drawback [8]. It, however, lowers the effectiveness of laser radiation application. Another variant for improvement of the quality of laser-MIG welding of 5083 alloy can be the process of welding from two sides, which is more suitable for joining thicknesses greater than 10 mm [9].

Thus, there is an urgent task of studying the features of the process of welding the known structural aluminium alloys is particular, of fifth series, with application of a consumable electrode arc and laser radiation. Here, it is important to consider the factors of improvement of the efficiency of application of radiation with wave length of the order of 1.06 μm. The 5083 alloy or 1561 alloy of up to 10 mm thickness close to it can be considered as the studied alloys [10].

PURPOSE AND OBJECTIVE OF THE STUDIES

The purpose of the work is to analyze the possibilities of improvement of process effectiveness and reduction of the specific energy input into the metal in

Table 1. Chemical composition of 1561 alloy, wt.%

Al	Mn	Si	Fe	Cu	Zn	Zr	Mg	Be
Base	0.8–1.1	≤0.4	≤0.4	≤0.1	≤0.2	0.02–0.12	5.5–6.5	0.0001–0.0003

consumable electrode pulsed-arc welding of 1561 aluminium alloy (P-MIG), due to involvement of laser radiation of the near infrared spectrum range in the process.

Solving the following tasks is proposed to achieve this purpose:

1. Analyze the interaction of arc and laser energy sources during welding of 1561 alloy and the influence of laser radiation on the features of P-MIG welding.
2. Analyze the influence of the change of laser radiation power on weld formation, change of the weld cross-sectional area and other parameters of P-MIG process of welding 1561 alloy.
3. Compare the obtained results of P-MIG welding of 1561 alloy without application of laser radiation and with its application.

MATERIALS, EQUIPMENT AND METHODS OF INVESTIGATION

The following investigation procedure was selected to achieve the defined purpose of the work: selection of parameters of the mode of P-MIG welding of 1561 aluminium alloy 6 mm thick by the criterion of satisfactory formation of the weld, investigation of the influence of addition of focused laser radiation (wave length $\lambda = 1.06$ μm) on the process of P-MIG welding, comparison of penetration of 1561 alloy plates ($\delta = 6$ mm) at P-MIG welding with and without addition of laser radiation, selection of parameters of the mode of laser-P-MIG welding of 1561 alloy ($\delta = 6$ mm) by the criterion of satisfactory formation of the weld, analysis of the obtained results by macrosections of weld cross-section, determination of the prospects of application of focused laser radiation ($\lambda = 1.06$ μm) together with consumable electrode pulsed arc in welding alloys of Al–Mg system.

In order to conduct the experiments, samples of 1561 alloy of 300×100×6 mm size were used in the work. Chemical composition of 1561 alloy is given in Table 1. Wire from the same alloy of 1.2 mm diameter was used as the consumable electrode.

Experiments were conducted by the scheme proposed in work [11]. According to this scheme, a laboratory facility was selected, based on a three-coordinate manipulator, which was used to conduct P-MIG and laser-P-MIG welding (Figure 1). Used for this purpose was an original welding head, which integrated the laser and arc components. During performance of studies on P-MIG welding the arc torch was installed upright on the sample, and in the studies of laser-P-MIG welding the axis of the focused laser beam was directed normal to the sample, and the arc torch was located ahead in the direction of welding at a certain angle (Figure 1, *a*). Used as the shielding gas was argon with flow rate of 12–20 l/min. Radiation of up to 4.0 kW power was supplied from Nd:YAG laser, using optical fibre of 400 μm diameter (up to 0.5 mm diameter of focusing spot). Fronius TPS-2700 power source with reserved polarity current of about 300 Hz was used as the power source for P-MIG process.

Sample welding was performed without edge preparation. The angle of inclination of the axis of focused laser radiation to the metal being welded was equal to 81°, and the angle of inclination of the arc torch was 55°. The weld root was formed on a variable backing from stainless steel with a forming groove of 1.5–2.1 mm depth.

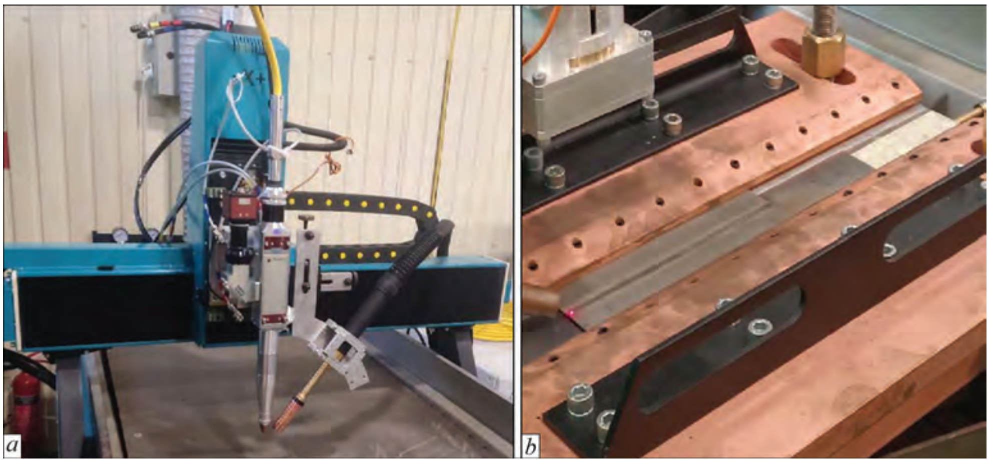

Figure 1. Facility (*a*) for conducting experiments on laser-P-MIG welding and clamp (*b*) with the sample after welding

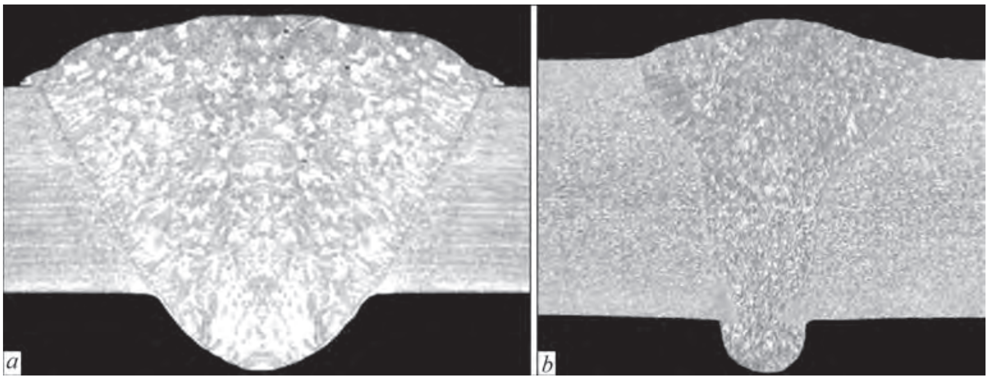

Figure 2. Macrostructure of welds produced by different processes of welding 1561 alloy (δ = 6 mm): *a* — P-MIG ($I \approx 200$ A; U = = 22.5 V; V = 0.42 m/min; $E_{MIG} \approx 4.8$ kJ/cm); *b* — laser-*P*-MIG welding (P = 3.0 kW; I = 75 A; U = 17 V; V = 1.0 m/min; E_{Σ} = 2.4 kJ/cm)

Welding was followed by making transverse sections of the samples, which were used further on to prepare macrosections. The geometrical parameters of the welds (width *B*, reinforcement height *a*, penetration depth *h*, cross-sectional area *S*) was determined on these macrosections with the accuracy of ±0.1 mm. The number and diameter of pores and voids in the welds were also assessed. When preparing the macrosections, the weld structure was revealed by chemical etching in the solution, which consisted of three acids — $HCl:HNO_3:HF$ in the proportion of 18:4:1. The weld microstructures were revealed in keeping with the recommendations of work [12]. The produced structures were studied in Neophot-32 microscope with the magnifications of ×50–1000. Mechanical testing for static uniaxial tension was conducted in keeping with the requirements of GOST 6996–66 with application of universal servohydraulic test system MTS 318.25 (Material Test System, USA) with the maximal force of 250 kN.

RESULTS OF INVESTIGATION OF ALUMINIUM ALLOY WELDING

Investigations were conducted by butt welding without edge preparation of 1561 aluminium alloy samples of the selected size. Here, the following ranges of welding mode parameter variation were chosen:

- P-MIG welding — welding current I = 100–= 200 A, arc voltage U = 16–24 V, process speed V = = 0.42; 0.5; 0.75; 1.0 m/min, filler wire feed rate V_w = = 4–12 m/min;
- laser-P-MIG welding — radiation power P = = 1–4 kW; process speed V = 0.5; 0.75; 1.0 m/min, ranges of other mode parameters are similar to P-MIG welding.

Values of energy inputs of the processes of metal welding from one side were calculated by the following formulas:

- P-MIG welding $E_{MIG} = 0.72IU/V$, kJ/cm, where 0.72 is the effective efficiency of a consumable electrode arc in argon [13, 14];
- laser welding $E_{las} = 0.75P/V$, kJ/cm, where 0.75 is the effective efficiency of welding by Nd:YAG laser [15];
- laser-P-MIG welding $E_{\Sigma} = E_{las} + E_{MIG}$.

First, the criterion of weld formation quality was used to select the mode of P-MIG welding (Figure 2, *a*). After that the mode of laser-P-MIG welding was selected in a similar way (Figure 2, *b*). Comparison of these welds showed that in the case of application

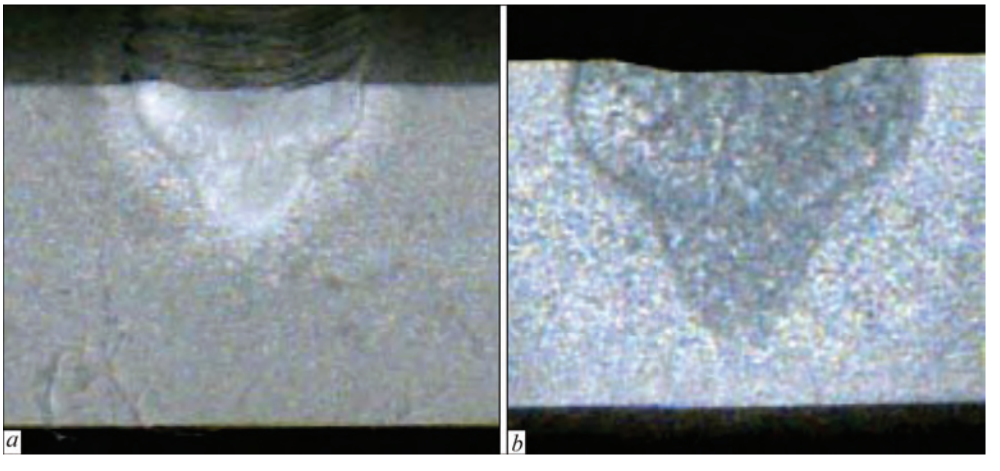

Figure 3. Macrostructure of weld deposits produced by laser welding of 1561 alloy (δ = 6 mm): *a* — P = 3.0 kW; V = 0.6 m/min; $E_{las} \approx 2.3$ kJ/cm; *b* — P = 4.0 kW; V = 0.5 m/min; $E_{las} \approx 3.6$ kJ/cm

Table 2. Geometrical shape of weld deposits in 1561 alloy (δ = 6 mm), depending on welding speed and electrode wire feed rate in P-MIG and laser-P-MIG processes

Welding modes		P-MIG welding	Laser-P-MIG welding (*P* = 4 kW)
Welding speed, m/min	Wire feed rate, m/min		
0.5	7.5	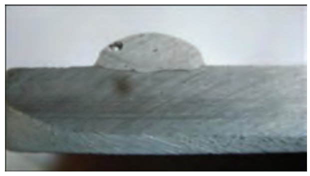	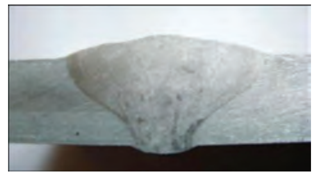
	8.3		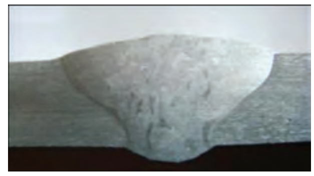
0.75	8.3	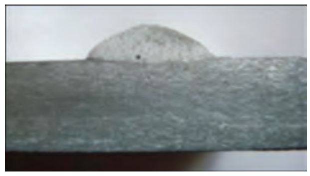	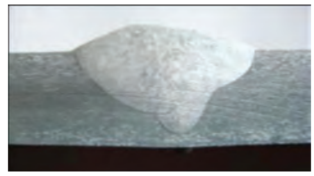
	9.3		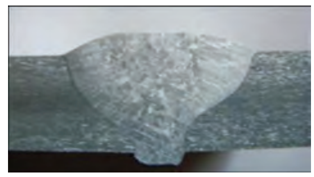
1.0	10.9		
	12.2		

of laser-P-MIG welding the welds is narrowed ~1.7 times. Further studies revealed that the welds are narrowed 1.5–2.0 times on average. Here, the welding energy input decreases approximately 2 times, compared to P-MIG welding, and the welding speed is increased more than 2 times. Such a result is indicative of the good prospects for replacement of P-MIG welding by laser-P-MIG welding and the need for a more detailed comparison of these processes.

An attempt to perform laser welding of 1561 alloy (δ = 6 mm) revealed problems with achievement of complete penetration, related to insufficient power density of the used Nd:YAG-laser, the radiation of which was focused into a spot of approximately 0.5 mm diameter. More over, the need to use filler material to eliminate weld sagging and to form upper reinforcement was determined (Figure 3).

It was found that under the conditions of P-MIG process in the range of welding speeds of 0.5–0.7 m/h and of wire feed rates of 7.5–9.3 m/min, it was not possible to achieve complete penetration of 6 mm 1561 alloy. At the same time, at the same modes the hybrid process of laser-P-MIG welding allows achieving complete penetration of the welded metal due to the availability of focused laser radiation of 4 kW power (Table 2).

More over, in addition to the obvious influence of laser radiation on the penetration depth and weld formation, its influence on the arc voltage and welding current was established during performance of technological studies. It was found that irrespective of the wire feed rate (in the range from 7.5 to 13.2 m/min) laser radiation of 4 kW power increases the arc voltage by 1–2 V (and the arc length, accordingly), and

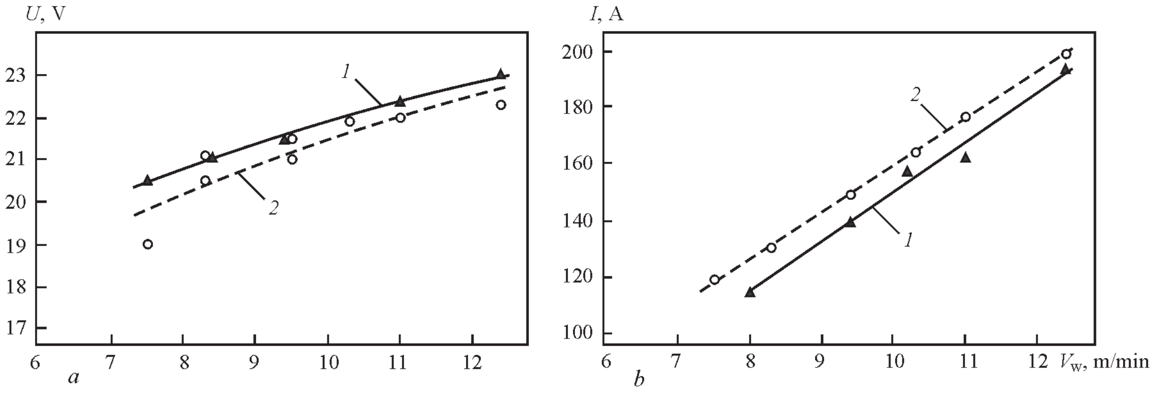

Figure 4. Dependencies of the change in arc voltage U, V and welding current I, A on electrode wire feed rate $V_{w,}$ m/min at laser-P-MIG (*1*) welding with 4 kW laser radiation and at P-MIG welding (*2*)

reduces the welding current by 10–15 A (Figure 4). With increase of laser radiation power from 1 up to 4 kW at unchanged electrode wire feed rate, the same dependence of increase of arc voltage and decrease of welding current (Table 3) is also observed. Here, an increase of the total $h + a$ value (penetration depth h + weld reinforcement height a) and weld width B at laser-P-MIG welding is found compared to P-MIG welding (Figure 5).

Preliminary studies, conducted at PWI showed [16] that with current increase in inert-gas consumable electrode welding the average temperature of

Table 3. Macrostructures of weld deposits, produced at P-MIG and laser-P-MIG welding of 1561 aluminium alloy (δ = 6 mm) (V = = 0.5 m/min; V_w = 8.3 m/min)

Welding current, I, A	Arc voltage U, V	Radiation power, P, kW	Result
135	18.7	0	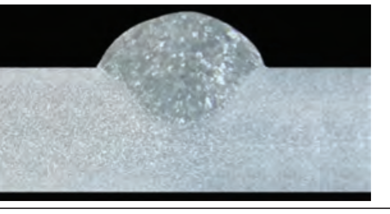
135	18.7	1	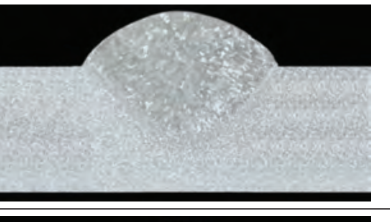
126	18.6	2	
130	20.0	3	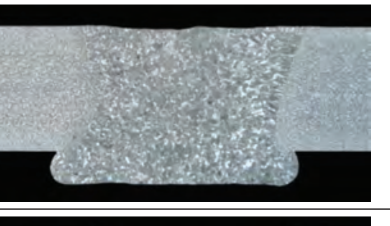
128	20.5	4	

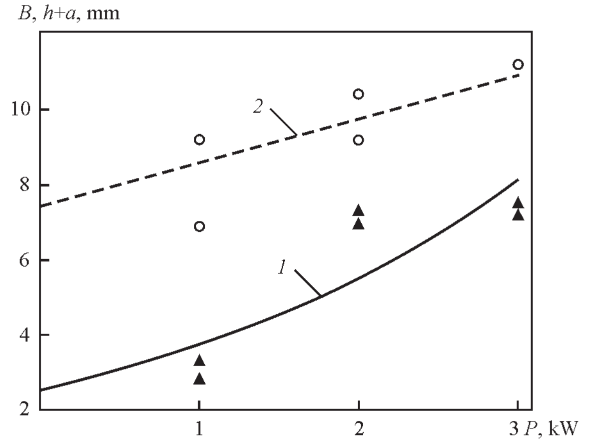

Figure 5. Influence of the change of laser power *P*, kW at laser-P-MIG welding (V = 0.5 m/min; V_w = 8.3 m/min) of 1561 alloy (δ = 6 mm) on increase of the total value of penetration depth *h* with reinforcement height *a* (*1*) and weld width *B* (*2*)

electrode metal drops is increased, reaching the values of boiling temperature of the aluminium alloy, from which the wire is made. Here, evaporation of metals with a comparatively low temperature of vapour formation, such as magnesium, lithium, zinc, etc occurs. Lowering magnesium content in the weld metal by one percent leads to decrease of the joint strength by 10–20 MPa. Conducted investigations showed that at P-MIG welding in the studied current range magnesium content in the weld metal can decrease by up to 25 % compared to the data in Table 1, and in the case of laser-P-MIG welding — by up to 15 %. It is probable that this is related to a considerable (up to 3 times) reduction of the weld pool volume.

The high average temperature of electrode metal drops in welding with consumable electrode of 1561 grade (irrespective of shielding gas composition) leads to evaporation of alloying elements and working zone contamination by welding aerosols of a complex chemical composition, which contain a number of toxic solid-phase components, namely Al_2O_3, MgO and MnO_2. Determination of the quantity of aerosols was performed by the following procedure. Air from

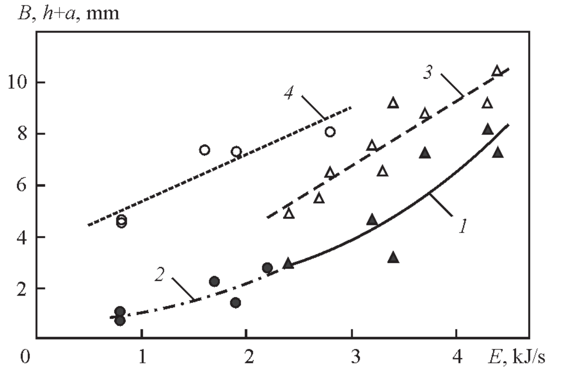

Figure 6. Influence of energy input *E*, kJ/cm of the processes of welding 1561 alloy (δ = 6 mm) on the total value of penetration depth *h* with reinforcement height *a* (*1*, *2*) and weld width *B* (*3*, *4*): *1*, *3* — laser-P-MIG (P = 4 kW); *2*, *4* – P-MIG

the welding zone at 20 cm distance from the arc was sampled with electric aspirator of 822 model with 12–15 l/min rate through preloaded AFA-VP-20 filters. The quantity of solid aerosols in the working zone air was measured by the gravimetric method. Al_2O_3, MgO and MnO_2 content was determined by the procedure described in work [17].

The total quantity of aerosols at P-MIG welding depends, primarily, on the density of welding current on the electrode wire. The higher the current density, the greater the quantity of aerosols formed around the weld pool. In the studied mode range, the current density was 50–90 A/ mm^2, here the concentrations of the respective welding aerosols were as follows: $K_{Al_2O_3}$ = = 125–145 mg/m^3, K_{MgO} = 14–17 mg/m^3, K_{MnO_2} = 1.9–2.2 mg/m^3. In laser-P-MIG welding no changes in the concentration of the above-mentioned welding aerosols were found.

In hybrid laser-MIG process the manifestation of the glow of focused laser radiation in the concentrated aerosol environment around the area of welding arc impact is very well observed. With increase of the wire melting rate (welding current), the number of electrode metal drops and volume of products evaporating from them become greater. It increases the density of gas environment in the near-cathode region. More over, the weld pool on aluminium alloys has the form of a kind of mirror, which increases in size with increase of welding current. It causes greater losses of laser radiation in a heterogeneous drop-aerosol environment around the pool and enhances its reflection from the pool proper. This results in reduction of the fraction of absorbed laser radiation and effective laser power, which acts directly on the metal being welded, i.e. the efficiency of the laser component of laser-P-MIG welding process is decreased. It leads to reduction of the penetration depth and change of geometrical parameters of the formed welds, accordingly.

Investigations of the influence of electrode wire feed rate on the geometrical parameters of weld deposits in P-MIG and laser-P-MIG welding showed the following. At the same welding speeds (V = 0.5 m/min) and wire feed rates (V_w = 7.5–9.3 m/min) the hybrid laser-P-MIG process allows increasing the weld width by 50–60 % compared to P-MIG at simultaneous reduction of reinforcement height by 10–60 % (in keeping with increase of V_w value). Similar dependencies are observed also at high welding speeds, but at smaller absolute values of the geometrical parameters of welds.

As shown by the conducted studies, introduction of laser radiation of power *P* into P-MIG process leads to increase of penetration depth (Figure 5). However, comparison of energy inputs of P-MIG and laser-P-

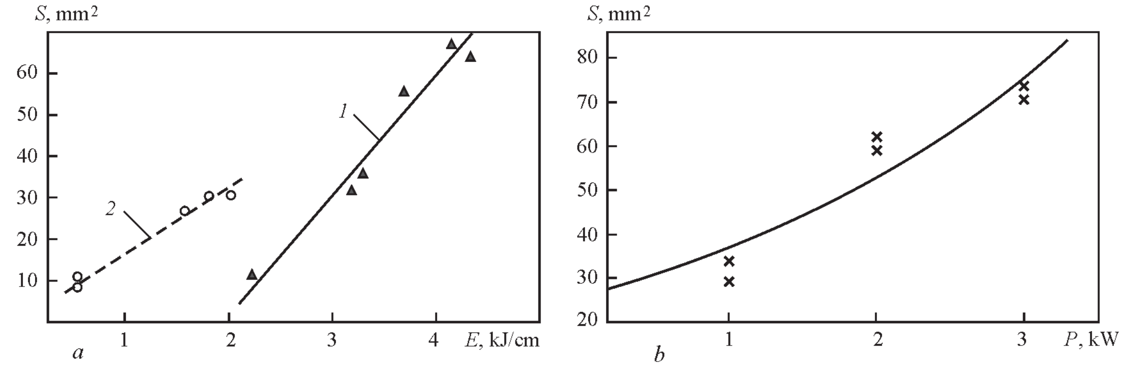

Figure 7. Influence of energy input *E*, kJ/cm (*a*) and laser radiation power *P*, kW (*b*) on area *S*, mm^2 of weld cross-section at laser-P-MIG welding of 1561 alloy (δ = 6 mm)

MIG welding shows that the process of increase of penetration depth (more exactly total $h + a$ value) is continuous and has a common tendency (Figure 6). In keeping with this tendency, increase of $h + a$ value is directly proportional to the welding energy input. Instead, the change of width of the welds and their cross-sectional area depends on the availability of laser radiation. So, at laser-MIG-welding with the same energy input the weld width decreases by 30–40 %, compared to weld width at P-MIG welding (Figure 6), which accounts for approximately three times reduction of the remelted metal area in this case (Figure 7, *a*). At the same time, increase of the remelted metal area with increase of laser power P at laser-P-MIG welding (Figure 7, *b*) is indicative of increase of penetration depth due to radiation impact.

As regards the characteristic weld defects in the form of inner pores and voids, it is not difficult to reduce their quantity and dimensions to acceptable level in the case of application of preliminary scraping of the edges and chemical etching of the electrode wire, as well as ensuring a reliable gas protection of the weld pool. Under the conditions of conducting the experiments, inner pores of 0.2–0.8 mm diameter were observed in the quantity of the order of 5–10 pcs/100 mm of the weld. Cracking susceptibility when producing the joints by the studied welding processes was not established. Investigations of microstructures of welds produced by laser, P-MIG and laser-P-MIG welding showed the dependence of weld structure on the welding process, which can be determined through the dendritic parameter (Figure 8). In the case of laser welding, the dendritic parameter is equal to 8 μm (Figure 8, *a*), at laser-P-MIG welding is it increased to 10 μm, and at P-MIG welding it is equal to 13–15 μm (Figure 8, *c*).

Microstructure of weld metal with all the studied welding processes predominantly depends on the welding method and mode. The weld metal structure is determined by grain shape and dimensions and their inner structure, as well as the shape, dimensions and location of chemical compounds, precipitating during crystallization. At close dimensions of the grains produced by laser-P-MIG and P-MIG welding, the dendrite branches can be both thin (in the case of laser-P-MIG, Figure 8, *b*), and thick (at P-MIG, Figure 8, *c*), and eutectic inclusions can be fine or coarse, respectively.

The formed structure influences the mechanical properties of the produced joints in an appropriate way. Static tensile testing showed that P-MIG welding allows reaching values of temporary fracture resistance of 314–323 MPa, and laser-P-MIG welding — 327–336 MPa. In all the cases, fracture occurred through the zone of weld fusion with base metal. Taking into account base metal strength (~350 MPa) it can be assumed that P-MIG welding ensures joint strength at the level of 90–92 %, and laser-P-MIG — at the level of 93–96%.

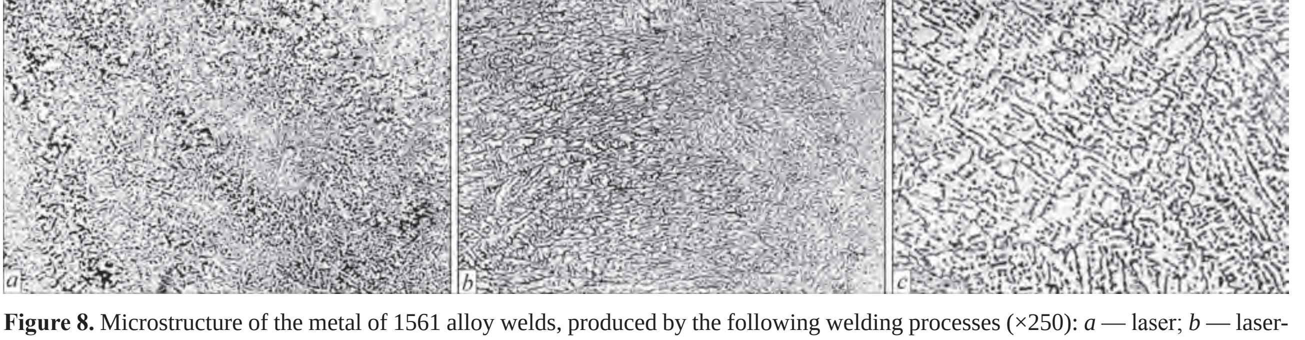

Figure 8. Microstructure of the metal of 1561 alloy welds, produced by the following welding processes (×250): *a* — laser; *b* — laser-P-MIG; *c* — P-MIG

DISCUSSION OF THE RESULTS OF STUDYING THE ALUMINIUM ALLOYS

Experiments show that at combination of the laser and P-MIG welding processes into one common process, the influence of focused laser radiation is primarily realized through creation of the keyhole, and the influence of consumable electrode arc — through improvement of absorption of laser radiation, creating a pool of a certain width, adding metal and formation of welds with certain geometrical parameters. With increase of the power of laser and arc components of the common process the density of evaporation from the weld pool and of spatter ejection from it are increased. It leads to increase of concentration of harmful welding aerosols and lowering of laser radiation efficiency due to its scattering, reflection from the pool and other power losses. In its turn, P-MIG welding is characterized by two times higher energy input and approximately 2–3 times greater weld width than laser-P-MIG welding (Figure 2), which may lead to greater values of the parameters of residual stress-strain state of welded structures. However, correct selection of the mode parameters can ensure acceptable results at application of each of the considered processes.

One of the most important factors, influencing the penetration depth at laser-P-MIG welding, is the ratio of powers of the laser and arc components and the process speed. So, in welding with the speed of 60 m/h, increase of electrode wire feed rate from 10.9 to 12.2 m/min (from I = 162 A, U = 22.4 V to I = = 194 A, U = 23 V, respectively) almost did not influence the increase of penetration depth, but increased the weld width from B = 10.1 mm to B = 13.5 mm (Table 2). This is associated with filling of the keyhole with electrode wire liquid metal, which is performed by the drop method and is an antiphase self-oscillation of the keyhole. In other cases, for instance, at laser-P-MIG welding at the speed of 45 m/h, drop transfer of electrode metal coincides with self-oscillation of the keyhole and promotes a considerable increase of penetration depth at increase of electrode wire feed speed from 8.3 (I = 123 A, U = 21.1 V) up to 9.3 (I = 142 A, U = 21.1 V) m/min (Table 2).

Increase of arc voltage with simultaneous reduction of welding current under the influence of laser radiation at P-MIG welding (Figure 4), is, primarily, associated with increase of ionization of the near-cathode region of the welding arc by radiation and with the respective change of the arc volt-ampere characteristics. Moreover, deepening of the weld pool due to formation of a keyhole by focused laser radiation leads to a certain elongation of the arc, causing an increase of arc voltage (to 0.5–1.0 V). At the same time, additional ionization of the zone of arc column impact can lead to a certain (~10 A) lowering of welding current. This tendency is directly proportional to increase of laser radiation power, and it becomes noticeable at its value above 1 kW at arc power of the order of 2 kW.

Absence of increase of welding aerosol evolution at transition from P-MIG to laser-P-MIG welding can be associated with two processes, occurring under the impact of laser radiation. On the one hand, the influence of laser radiation power promotes increase of evaporation of aluminium, magnesium and other elements and formation of such aerosols as Al_2O_3, MgO and MnO_2. On the one hand, under the impact of laser radiation reflected from the weld pool the anode region of electrode wire is additionally heated and becomes larger (i.e. the surface of the metal drop formed at the electrode wire tip, which is covered by the arc discharge, becomes greater). Here, the current density decreases, lowering the intensity of welding aerosol formation at the same time.

The main factor, which determines the type of weld microstructure, is the cooling rate at crystallization. Therefore, to assess the structure, the dendritic parameter was selected as the main index of the process of change of weld metal crystallization rate (Figure 8). The dimensions of the dendritic parameter depend on the ratio of laser and arc powers. In the studied case, the dendritic parameter of laser-P-MIG welding (10 μm) was somewhat closer to the case of laser welding (8 μm), than to that of P-MIG process (13–15 μm), which was attributable to higher welding speed (1.0 m/min), lower energy input (~ 2.4 kJ/cm). Such a decrease of the dendritic parameter can account for increase of the level of mechanical properties of the joints produced by laser-P-MIG welding (increase of power by 3–4 %).

CONCLUSIONS

1. It was established that at laser-P-MIG welding of 1561 alloy the influence of the arc energy source promotes improvement of laser radiation absorption and sound formation of weld reinforcement, and the laser source influence leads to increase of penetration depth due to keyhole formation, and to lowering of current density in the arc anode region on electrode wire that reduces welding aerosol evolution. Here, the effectiveness of laser radiation can be decreased because of power losses with spattering of metal drops from the weld pool and keyhole filling with electrode wire liquid metal, which can be prevented by selection of the ratio of welding speed and laser and arc powers.

2. The action of focused laser radiation on P-MIG process of welding 1561 alloy becomes noticeable

starting from 1 kW, and it is manifested in exponential increase of penetration depth and cross-sectional area of welds with power increase. Increase of laser radiation power leads to arc voltage rising from 1–2 V at 2 kW up to 0.1–0.3 V at 4 kW with simultaneous decrease of welding current from 13–15 A to ~6 A, respectively, at welding speed of 0.5 m/min.

3. It was established that application of P-MIG process for welding 6 mm 1561 alloy requires energy input of 4.5–5.0 kJ/cm and allows formation of a regular structure of weld metal with dendritic parameter of 15 μm and joint strength equal to 90–92 % of base metal strength. Introduction of focused radiation of 3 kW Nd:YAG laser into the welding process enables reducing the energy input two times, resulting in dendritic parameter lowering to 10 μm, and joint strength increasing to 93–96 % of base metal strength.

REFERENCES

1. Benedyk, J.C. (2010) 3 — Aluminium alloys for lightweight automotive structures. In: *Woodhead Publishing Series in Composites Science and Engineering, Materials, Design and Manufacturing for Lightweight Vehicles*, 79–113. Ed. by P.K. Mallick. Woodhead Publishing. DOI: https://doi.org/10.1533/9781845697822.1.79
2. Sun, Y. (2023) The use of aluminium alloys in structures: Review and outlook. *Structures*, 57(**5**), 105290. DOI: https://doi.org/10.1016/j.istruc.2023.105290
3. Hung, F.-S. (2020) Design of lightweight aluminium alloy building materials for corrosion and wear resistance. *Emerging Materials Research*, 9(**3**), 750–757. DOI: https://doi.org/10.1680/jemmr.19.00177
4. Ambriz, R.R., Mayagoitia, V. (2011) *Welding of aluminium alloys.* In: *Recent Trends in Processing and Degradation of Aluminium Alloys*, **516**, 63–86. Ed. by Prof. Zaki Ahmad. DOI: https://doi.org/10.5772/18757
5. Khaskin, V.Y. (2013) Development of laser welding of aluminium alloys at the E.O. Paton Electric Welding Institute. *The Paton Welding J.*, **5**, 51–55.
6. Bushma, A.I. (2015) State-of-the-art of hybrid laser-plasma welding (Review). *The Paton Welding J.*, **8**, 18–25. DOI: https://doi.org/10.15407/tpwj2015.08.04
7. Bunaziv, I., Akselsen, O. M., Salminen, A., Unt, A. (2016) Fiber laser-MIG hybrid welding of 5 mm 5083 aluminium alloy. *J. Materials Proc. Technology*, **233**, 107–114. DOI: https://doi.org/10.1016/j.jmatprotec.2016.02.018
8. Sánchez-Amaya, J. M., Pérez, T. D., Rovira, L. G., Botana, J. (2009) Laser welding of aluminium alloys 5083 and 6082 under conduction regime. *Appl. Surface Sci.*, 255(**23**), 9512–9521. DOI: https://doi.org/0.1016/j.apsusc.2009.07.081
9. Jiang, Z., Hua, X., Huang, L. et al. (2018) Double-sided hybrid laser-MIG welding plus MIG welding of 30-mm-thick aluminium alloy. *Int. J. Adv. Manuf. Technol*., **97**, 903–913. DOI: https://doi.org/10.1007/s00170-018-1997-7
10. Babych, O.A., Korzhyk, V.M., Grynyuk, A.A. et al. (2020) Hybrid welding of aluminium 1561 and 5083 alloys using plasma-arc and consumable electrode arc (Plasma-MIG). *The Paton Welding J.*, **7**, 11–22. DOI: https://doi.org/10.37434/tpwj2020.07.02
11. Krivtsun, I.V., Khaskin, V.Yu., Korzhik, V.N., Luo, Ziyi (2015) Industrial application of hybrid laser-arc welding (Review). *The Paton Welding J.*, **7**, 41–46. DOI: https://doi.org/10.15407/tpwj2015.07.07
12. (2018) *Encyclopedia of aluminium and its alloys*. 2 Vols Ed. by G.E. Totten et al., 1st Ed. Boca Raton, CRC Press. DOI: https://doi.org/10.1201/9781351045636
13. DuPont, J.N., Marder, A.R. (1995) Thermal efficiency of arc welding processes. *Welding J.*, **74**, 406–416.
14. Hälsig, A., Mayr, P. (2013) Energy balance study of gas-shielded arc welding processes. *Welding in the World, Le Soudage dans le Monde*, 57(**5**). DOI: https://doi.org/10.1007/s40194-013-0073-z
15. De Oliveira, A.F.M., dos S. Magalhães, E., dos S. Paes, L.E. et al. (2023) A thermal analysis of laser beam welding using statistical approaches. *Processes*, 11(**7**). DOI: https://doi.org/10.3390/pr11072023
16. Levchenko, O.G., Mashin, V.S. (2003) Sanitary-hygienic characteristic of process of consumable electrode inert-gas welding of AMg6 aluminium alloy. *The Paton Welding J*., **1**, 46–48.
17. Cole, H., Epstein, S., Peace, J. (2007) Particulate and gaseous emissions when welding aluminium alloys. *J. of Occupational and Environmental Hygiene*, 4(**9**). DOI: https://doi.org/10.1080/15459620701516162

ORCID

Y. Zhao: 0000-0001-9471-4490,
X. Wang: 0009-0003-3423-2547,
Z. Liu: 0000-0002-0074-9666,
V.Yu. Khaskin: 0000-0003-3072-6761

CONFLICT OF INTEREST

The Authors declare no conflict of interest

CORRESPONDING AUTHOR

V.Yu. Khaskin
Guangdong Provincial Key Laboratory of Advanced Welding Technology, China-Ukraine Institute of Welding, Guangdong Academy of Sciences, Guangzhou, 510650, China.
E-mail: khaskin1969@gmail.com

SUGGESTED CITATION

Y. Zhao, X. Wang, Z. Liu, V.Yu. Khaskin (2024) Effectiveness of the influence of solid-state laser radiation on the process of pulsed-arc welding of aluminium alloy 1561. *The Paton Welding J.*, **6**, 29–37.
DOI: https://doi.org/10.37434/tpwj2024.06.04

JOURNAL HOME PAGE

https://patonpublishinghouse.com/eng/journals/tpwj

Received: 30.04.2024
Received in revised form: 05.06.2024
Accepted: 22.07.2024